Trajectory generation for a fixed-wing UAV by the potential field method

Amar BENGHEZAL[(1)], Rabah LOUALI[(2)],
Abedelouahab BAZOULA[(3)]
École Militaire Polytechnique, Laboratoire Robotique,
BP 17, Bordj El Bahri, Algiers, Algeria
amar.benghezal@gmail.com[(1)],
rabah.louali@gmail.com[(2)],
abdelouahab.bazoula@gmail.com[(3)]

Taha CHETTIBI[(4)]
École Militaire Polytechnique, Laboratoire
Mécanique des structures,
BP 17, Bordj El Bahri, Algiers, Algeria
tahachettibi@gmail.com[(4)]

***Abstract* — In this work we propose an online 3D trajectory generation based Artificial Potential Field method (APF) for fixed-wing UAVs. The proposed approach uses a simplified dynamic model in order to ensure the feasibility of the generated trajectory by the real UAV. Simulations show the feasibility of the approach in the cases of waypoints navigation in both free environment and obstructed environment.**

***Index Terms* — UAV fixed-wings; Artificial potential field; 3D online trajectory generation; dynamic model.**

I. INTRODUCTION

Unmanned Aerial Vehicles (UAVs) that can be used in hazardous environments as a cost effective and safe alternative to manned aircrafts. Their applications are not limited to military missions, but they are also used in civilian applications such as search, rescue and environmental monitoring. A generic UAV mission involves navigating through a set of points specified a priori according to the scenario of the mission and environmental data [1]. The latter is generally hostile and uncertain. In addition, the uncertainties during execution of the mission may require online replanning (appearance of obstacles).

Compared with vertical takeoff and landing UAVs (VTOL), fixed-wing UAVs have the advantage of a simpler mechanical structure with a greater radius of action, altitudes and speed [2]. However, fixed-wing UAVs have a non-holonomic motion expressed by the bank to turn effect [2]. Furthermore the lift force, generated by the translational speed consequence of the engine propulsion (thrust), must be greater than the weight of the UAV to avoid stalling [2].

The trajectory generation consists of defining a set of paths, parameterized by time in order to accomplish a mission defined by waypoints respecting the environment constraints and the dynamic limitations of the mobile. The importance and complexity of the trajectory generation problem is reflected in the number of research activities in this field. Depending on the objectives of the mission, the generation of the trajectory can be done online or offline. Among works dealing with offline trajectory generation for UAVs, we cite [3] and [4] that generate a polygonal path from a graph using free configurations (Voronoï graph, visibility or probabilistic road maps). Works [1], [5], [6] and [7] use optimization methods to solve the problem of constrained trajectory generation (a set of splines is chosen optimally). Other researchers exploit Dubins and Bezier curves to solve the trajectory generation problem [8]-[11].

The artificial potential field (APF) is an online trajectory generation method [15]. It enables robots to navigate in an environment by avoiding fixed or mobile obstacles. It is widespread in mobile robotics due to its mathematical and algorithmic simplicity [12]-[14]. Other works generalize this method to the case of VTOL UAVs by generating 3D trajectories [17], [18]. However, few authors report the use of APF for fixed-wing UAVs [19] where authors require roll commands nil and they test the system in navigation mode to a non-zero altitude.

The contribution of this work is an online 3D trajectory generation based APF for a fixed-wing UAV. The proposed approach uses the UAV simplified dynamic model, to ensure the feasibility of the generated trajectory by the real UAV.

This paper is organized as follows: in the second section we present our approach, by giving the UAV model, a brief survey of the APF method and calculation of the necessary commands for the generation of the trajectory. The third section is devoted to the simulation results in the case of an environment without obstacles and with obstacles. Finally we end with a conclusion.

II. PROPOSED APPROACH

The proposed approach is represented by the block diagram of Fig.1.

The environment model and the UAV state are used to compute potential field forces. The UAV commands are computed basing on these latter, then inputted to the dynamic model, which outputs constitute the generated trajectory.

Sub blocks of the proposed approach will be explained in the following sub sections.

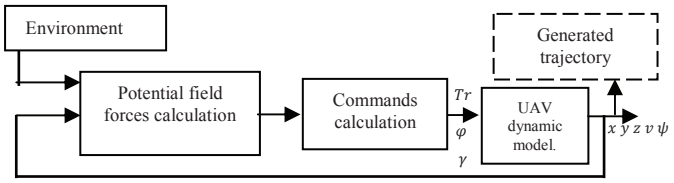

Figure 1.Block diagram of the proposed approach trajectory generation.

A. *UAV model*

The model of the UAV is developed in the inertial frame $R_I\{O_I, \vec{X}_I, \vec{Y}_I, \vec{Z}_I\}$. In addition to this frame, we define a frame linked to the body of the UAV $R_B\{O_B, \vec{X}_B, \vec{Y}_B, \vec{Z}_B\}$ where its origin is at the centre of gravity and $\vec{X}_B$ is along the longitudinal axis. Fig.2 shows frames and parameters used in the UAV model.

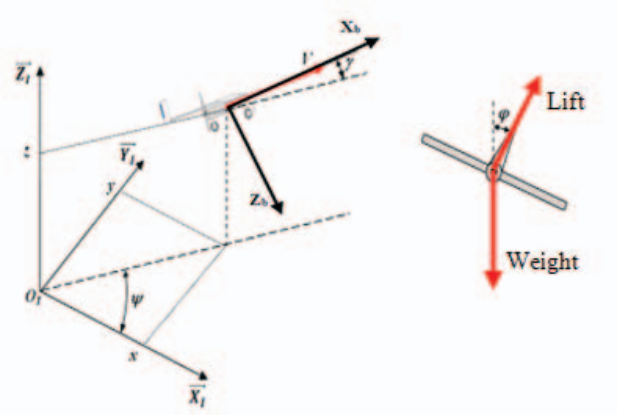

Figure 2.Frames and parameters of the UAV model.

We adopt the simplified dynamic model described by the nonlinear state space system (1)-(5) [1][20]. This model assumes that the earth is locally flat and that the UAV mass is constant. The state x, y, z, ψ and v are respectively the Cartesian coordinates, heading angle and longitudinal velocity of the plane. Commands are the thrust (T_r), the banking angle (φ) and the angle of attack (γ).

$$\frac{dv}{dt} = \frac{1}{m}(T_r - D) - gsin(\gamma) \quad (1)$$

$$\frac{d\psi}{dt} = \frac{gn}{v}\frac{sin(\varphi)}{cos(\gamma)} \quad (2)$$

$$\frac{dx}{dt} = vcos(\gamma)cos(\psi) \quad (3)$$

$$\frac{dy}{dt} = vcos(\gamma)sin(\psi) \quad (4)$$

$$\frac{dz}{dt} = vsin(\gamma) \quad (5)$$

The translational speed v is generated by the thrust as attested by (1). Bank to turn effect is expressed by (2).

The drag force D is calculated according to (6), where ρ is the air density, S is a reference area, n is the load factor and (C_{d0}, k) are parameters of the drag force. The UAV mass and gravity are m and g respectively.

$$D = 0.5\rho v^2 S C_{d0} + \frac{2kn^2(mg)^2}{\rho v^2 S} \quad (6)$$

The load factor n is the ratio of the lift force and the weight of the UAV expressed in (7). The stall speed v_{min} is calculated in the limiting case where the lift force is equal to the weight (8).

$$n = \frac{L}{mg} = \frac{0.5\rho C_L S v^2}{mg} \quad (7)$$

$$v_{min} = \sqrt{\frac{2mg}{\rho C_L S}} \quad (8)$$

The commands dynamics can be modeled by the first-order differential equations (9)-(11), where $\tau_t, \tau_\varphi, \tau_\gamma$ are time constants [20].

$$\frac{dT_r}{dt} = \frac{1}{\tau_t}(T_{rc} - T_r) \quad (9)$$

$$\frac{d\varphi}{dt} = \frac{1}{\tau_\varphi}(\varphi_c - \varphi) \quad (10)$$

$$\frac{d\gamma}{dt} = \frac{1}{\tau_\gamma}(\gamma_c - \gamma) \quad (11)$$

Commands of the UAV are saturated to avoid instability or to not exceed the limits set by the manufacturer. These limits are:

$T_{rmin} \leqslant T_r \leqslant T_{rmax}$	Engine physical limits
$\gamma_{min} \leqslant \gamma \leqslant \gamma_{max}$	Avoid stalling
$\varphi_{min} \leqslant \varphi \leqslant \varphi_{max}$	Avoid stalling
$v_{min} \leqslant v \leqslant v_{max}$	

v_{max} : Engine limit and v_{min}: Avoid stalling.

The model presented in this subsection includes the static and dynamic limits of the UAV. A trajectory generation based on this model will guarantee the achievability of this trajectory by real UAVs.

B. *Artificial Potentials Fields Method*

The basic concept of the method is to fill the mobile system workspace with artificial potential field, in which the mobile system is attracted to the goal position and repelled by the obstacles [15]. The combination of the attractive force toward the object position and the repulsive force of the obstacles provides secure trajectories towards the target point.

Attractive potential field

Let $q_0 = (x, y, z)$ is the current position of the UAV in space. The usual choice of attractive potential is the standard parabolic shape that is growing in quadrature with the distance to the goal, such as:

$$U_{att}(q_0) = \frac{1}{2}K_a d^2_{goal}(q_0) \quad (12)$$

Where $d_{goal} = \|q_0 - q_{goal}\|$ is the Euclidean distance between the current position of the UAV and target point q_{goal}, K_a is a scaling factor (attraction factor).

The attractive force in the approach of the APF method is the negative gradient of the attractive potential:

$$\overrightarrow{F}(q_0) = - \bigtriangledown U_{att}(q_0) = -K_a(q_0 - q_{goal}) \qquad (13)$$

Repulsive potential field

The repulsive potential allows the UAV to move away from the obstacle: It is important when the UAV is close to the obstacle and less influence when the UAV is far from it. Furthermore, we want that this potential does not affect the motion of the UAV when the latter is far enough away from obstacles.

Several forms of the repulsive potential of the obstacle are given in the literature. We adopt the form expressed by (14):

$$\overrightarrow{F}_i(q_0) = \begin{cases} e^{-k_{rep} d_{obs_i}(q_0)(q_0 - q_{obs_i})} & \text{if } d_{obs_i}(q_0) \leqslant d_0 \\ 0 & \text{if } d_{obs_i}(q_0) > d_0 \end{cases} \qquad (14)$$

Such as q_{obs} is the position of the obstacle, i is the number of the obstacle, $d_{obsi}(q_0)$ is the distance between UAV and the obstacle i, K_{rep} is a scaling factor (repulsion factor) and $d_0$is the minimum distance (threshold) of the influence of the obstacle.

The resultant force $\overrightarrow{R}$ is the sum of the repulsive force $\overrightarrow{F}_{rep}$ and the attractive force $\overrightarrow{F}_{att}$ (15):

$$\overrightarrow{R} = \begin{pmatrix} R_x \\ R_y \\ R_z \end{pmatrix} = \overrightarrow{F}_{att} + \overrightarrow{F}_{rep} \qquad (15)$$

The following section explains the calculation of the UAV commands based on the resultant force of the potential field $\vec{R}$.

C. Commands calculation

The application of (16), inspired by Newton's first law, allows the passage from forces field to desired velocities field $\overrightarrow{V} = [v_x \; v_y \; v_z]^T$.

$$\overrightarrow{R} - \lambda \overrightarrow{V} = m \frac{d\overrightarrow{V}}{dt} \lambda > 0, \qquad (16)$$

The coefficient λ is a positive factor that dampens the oscillation of the generated path.

The desired angle-of-attack and heading are calculated by using respectively (17) and (18) .

$$\gamma_c = atan\left(\frac{u_z}{\sqrt{u_x^2 + u_y^2}}\right) \qquad (17)$$

$$\psi_c = atan\left(\frac{u_y}{u_x}\right) \qquad (18)$$

In order to calculate the desired longitudinal velocity of the UAV v_c, we project velocities $\overrightarrow{U}$ in the reference related to the body of the UAV $R_B\{O_B, \overrightarrow{X}_B, \overrightarrow{Y}_B, \overrightarrow{Z}_B\}$using a transition matrix ${}^B T_i$. The latter is calculated in terms of the attitude of the UAV.

$$\overrightarrow{V}_c = {}^B T_i \, \overrightarrow{U} \qquad (19)$$

$${}^B T_i = \begin{bmatrix} C(\theta)C(\psi) & C(\theta)S(\psi) & -S(\theta) \\ -C(\theta)S(\psi) + S(\varphi)S(\theta)C(\psi) & C(\varphi)C(\psi) + S(\varphi)S(\theta)S(\psi) & S(\varphi)C(\theta) \\ S(\varphi)S(\psi) + C(\varphi)S(\theta)C(\psi) & -S(\varphi)C(\psi) + C(\varphi)S(\theta)S(\psi) & C(\varphi)C(\theta) \end{bmatrix}, \qquad (20)$$

C = cos, S = sin.

As fixed wing UAV translate according to the longitudinal speed, then:

$$v_c = \overrightarrow{V_c}.\overrightarrow{X_b} \qquad (21)$$

The desired thrust force (command) is calculated by (22), such that D is the drag force and ω_v is a bandwidth factor of command T_{rc}. The desired load factor and roll angle are given by (23) and (24)[20].

$$T_{rc} = D + \omega_v m(v_v - v) + mgsin(\gamma) \qquad (22)$$

$$n_c = \sqrt{a^2 + b^2} \qquad (23)$$

$$\varphi_c = tan^{-1}\left(\frac{b}{a}\right) \qquad (24)$$

Such as

$$a = \omega_\gamma v \frac{(\gamma_c - \gamma)}{g} + cos(\gamma); \; b = \omega_\psi v \frac{(\psi_c - \psi)}{g} cos(\gamma)$$

These commands are injected into the dynamic model of the UAV to generate the trajectory.

III. SIMULATION RESULTS

A. Go to the goal without obstacles

This section presents the simulation of the proposed approach applied for the UAV AEROSONDE [21] in the case of a mission defined by waypoints in environment without obstacles. The starting point of the UAV is q0=(-40,-40,0), and then passes through the crossing points (waypoints) following (q1=[60,60,5], q2=[60,-60,5], q3=[-60,60,20], q4=[-60,-60,20]) to form a path of the shape of number eight (switching an aim point to another). The parameters of the simulation are given in Table 1.

The resulting trajectory is shown in Fig.3. It is noted that the UAV passes through the points indicated above. The commands (Tr, φ and γ) (Fig.4-6) do not exceed their limitations given in Table 1. Note that in Fig. 4, 7 thrust and speed are above their minimum values (stall speed, the red line in Fig.7). From Fig.4 the thrust increases from zero (time of

take-off) then there is time when the thrust is constant (between same altitude crossing points), we note that the thrust is proportional to the altitude error.

Table 1. Parameters of the UAV Aerosonde.

Mass	M=13.5kg
Pitch angle min	γ_{min}= -20°
Pitch angle max	γ_{max}= +20°
Roll angle min	φ_{min}= -30°
Roll angle max	φ_{max}= +30°
Drag coefficient	C_{d0}=0.043
Reference area	S=1.5m^2
Lift coefficient	$C_L = 1.5$
Airdensity	$\rho = 1.211$ kg/m^3
Speed min	V_{min}=12ms^{-1}
Thrust max	Tr_{max}=200N

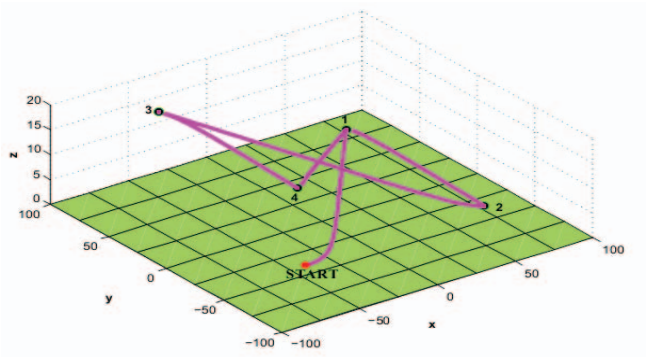

Figure 3. Trajectory generated without obstacles.

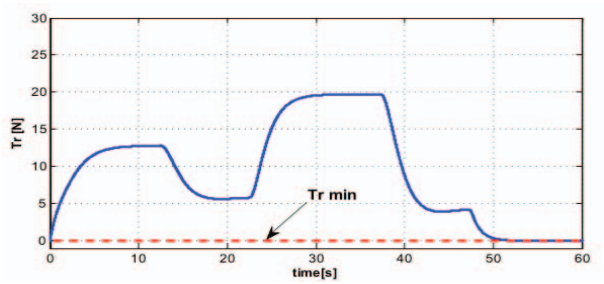

Figure 4. Evolution of the thrust force.

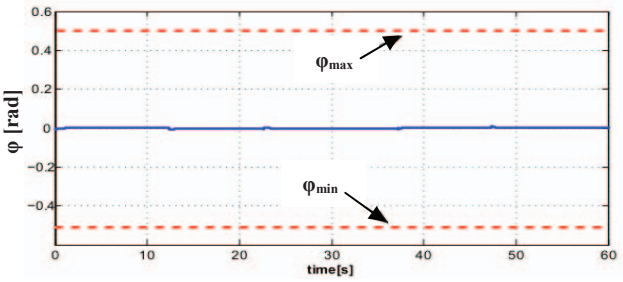

Figure 5. Evolution of roll angle.

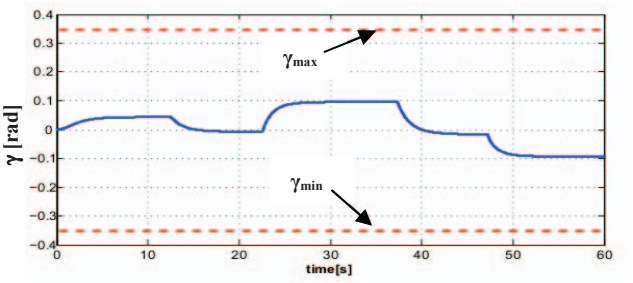

Figure 6. Evolution of angle of attack.

The change in the altitude of the UAV is logical, as we noted in Fig.6 that the angle of attack is constant when the aircraft generates a path between two points of the same elevation. Fig.5 and 6 confirm that the heading change is linked to roll change.

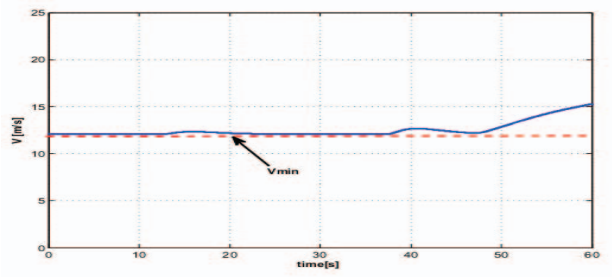

Figure 7. Evolution of speed.

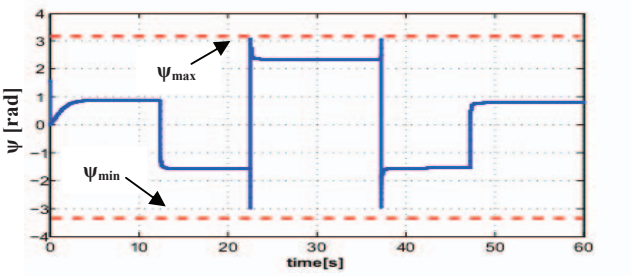

Figure 8. Evolution of yaw angle.

The evolution of the rotational dynamics of the UAV shows a feasible trajectory for the UAV fixed-wing.

B. Go to the goal with an obstacle

In this case, we simulate the same scenario as above (starting point and crossing points), but in an environment obstructed by an obstacle in the form of a hemisphere of coordinates (0, 0, 0) and radius of 15m. The simple shape of the obstacle does not detract from the generality of the proposed approach. Practically, the real obstacles are wrapped in simple geometric shapes. The generated trajectory is shown in Fig.9; we note that the UAV goes through all the points designated avoiding obstacle.

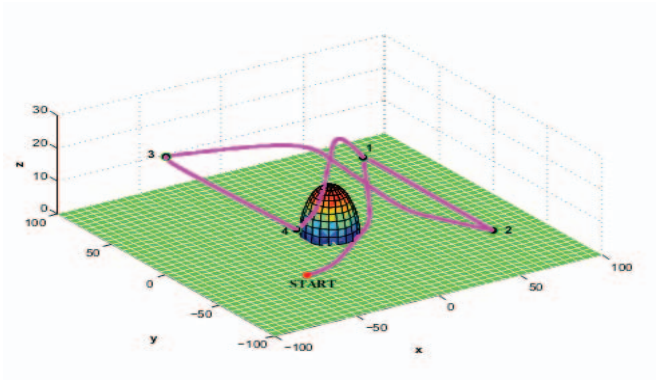

Figure 9.Trajectory generated with an obstacle.

The commands (Fig.10-12) for trajectory generation respect the limits of UAV shown in table 1. As we remarked in the Fig.10, 13 thrust and speed are greater than their minimum values. In figure 10 we note that the thrust is important that the thrust in the scenario without obstacle, and this because the UAV has encountered an obstacle in its path.

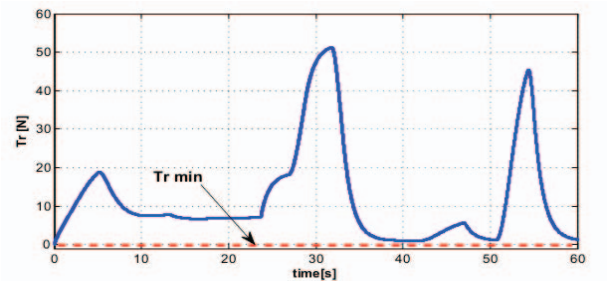

Figure 10.Evolution of the thrust force.

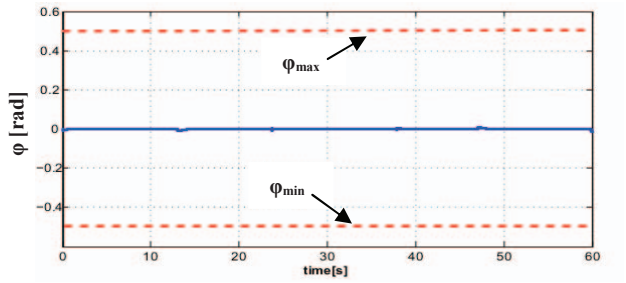

Figure 11.Evolution of roll angle.

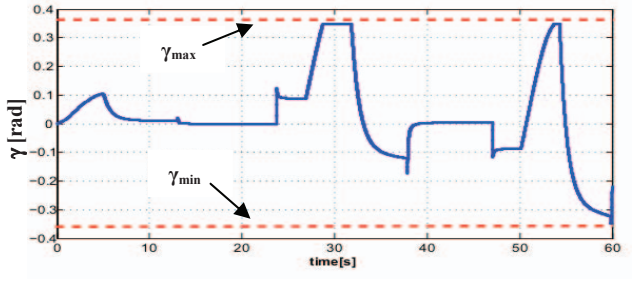

Figure 12.Evolution of angle of attack.

The angle of attack (fig .12) changes according to the meeting of the UAV with obstacle and it respect the limits shown in table 1.

In figure 13 we remarque that the speed changes according the change of the thrust (fig .10) with delay of time (see eq.1).

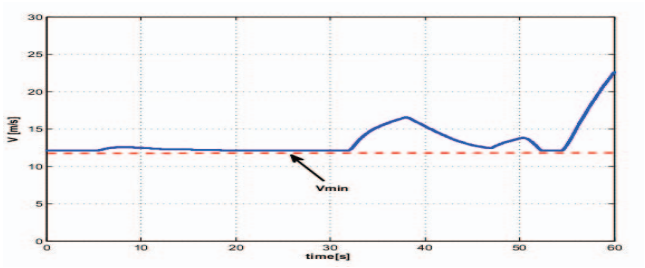

Figure 13.Evolution of speed.

The evolution of the rotational dynamics of the UAV shows a feasible trajectory for the UAV fixed-wing by the respect of the limits imposed in table1.

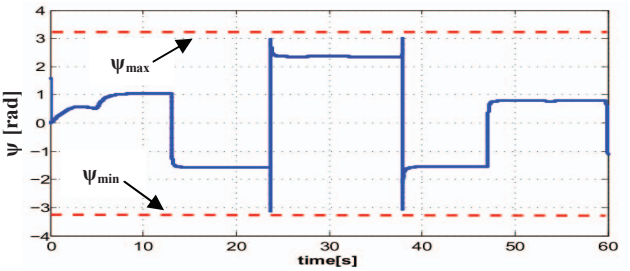

Figure 14.Evolution of yaw angle.

IV. CONCLUSION

We proposed in this paper an approach based on a potential field method for online 3D trajectory generation for fixed-wing UAVs. This method uses a simplified dynamic model in order to ensure the feasibility of the generated trajectory by the real UAV. The proposed approach has a mathematical structure and simple algorithms, simplifying its real-time implementation. Simulations show the feasibility of the trajectories in the cases of free environment and obstructed environment.

We plan to implement this approach in real UAV, with respecting of the real time constraints and extend this approach to UAV fleet.

REFERENCES

[1] T. Chettibi, "Generating near-optimal reference trajectories for small fixed-wing uavs," *International Journal of Robotics and Automation,* vol. 26, 2011.

[2] R. Louali*, et al.*, "Designing embedded systems for fixed-wing UAVs: Dynamic models study for the choice of an emulation vehicle," in *Multi-Conference on Systems, Signals & Devices (SSD), 2014 11th International*, 2014, pp. 1-6.

[3] Y. Kwangjin and S. Sukkarieh, "Real-time continuous curvature path planning of UAVS in cluttered environments," in *Mechatronics and Its Applications, 2008. ISMA 2008. 5th International Symposium on*, 2008, pp. 1-6.

[4] F. Scholer*, et al.*, "Generating approximative minimum length paths in 3D for UAVs," in *Intelligent Vehicles Symposium (IV), 2012 IEEE*, 2012, pp. 229-233.

[5] G. Brian*, et al.*, "Optimal Path Planning of UAVs Using Direct Collocation with Nonlinear Programming," in *AIAA Guidance, Navigation, and Control Conference and Exhibit*: American Institute of Aeronautics and Astronautics, 2006.

[6] G. Sanders and T. Ray, "Optimal offline path planning of a fixed wing unmanned aerial vehicle (UAV) using an evolutionary algorithm," in *Evolutionary Computation, 2007. CEC 2007. IEEE Congress on*, 2007, pp. 4410-4416.

[7] V. Roberge*, et al.*, "Comparison of Parallel Genetic Algorithm and Particle Swarm Optimization for Real-Time UAV Path Planning," *Industrial Informatics, IEEE Transactions on,* vol. 9, pp. 132-141, 2013.

[8] G. Ambrosino*, et al.*, "Algorithms for 3D UAV Path Generation and Tracking," in *Decision and Control, 2006 45th IEEE Conference on*, 2006, pp. 5275-5280.

[9] A. Neto*, et al.*, "Feasible path planning for fixed-wing UAVs using seventh order Bézier curves," *Journal of the Brazilian Computer Society,* vol. 19, pp. 193-203, 2013/06/01 2013.

[10] L. Yucong and S. Saripalli, "Path planning using 3D Dubins Curve for Unmanned Aerial Vehicles," in *Unmanned Aircraft Systems (ICUAS), 2014 International Conference on*, 2014, pp. 296-304.

[11] I. Lugo-Cardenas*, et al.*, "Dubins path generation for a fixed wing UAV," in *Unmanned Aircraft Systems (ICUAS), 2014 International Conference on*, 2014, pp. 339-346.

[12] S. Scherer*, et al.*, "Flying Fast and Low Among Obstacles: Methodology and Experiments," *The International Journal of Robotics Research,* vol. 27, pp. 549-574, 2008.

[13] A. Berry*, et al.*, "A Continuous Local Motion Planning Framework for Unmanned Vehicles in Complex Environments," *Journal of Intelligent & Robotic Systems,* vol. 66, pp. 477-494, 2012/06/01 2012.

[14] A. Bazoula*, et al.*, "Formation control of multi-robots via fuzzy logic technique," *International Journal of Computers, Communications & Control,* vol. 3, 2008.

[15] O. Khatib, "Real-time Obstacle Avoidance for Manipulators and Mobile Robots," *Int. Jour. of Rob. Research,* vol. 5(1), pp. 90-98, 1986.

[16] M. T. Wolf and J. W. Burdick, "Artificial potential functions for highway driving with collision avoidance," in *Robotics and Automation, 2008. ICRA 2008. IEEE International Conference on*, 2008, pp. 3731-3736.

[17] V. Erik de and S. Kamesh, "Cooperative Control of Swarms of Unmanned Aerial Vehicles," in *49th AIAA Aerospace Sciences Meeting including the New Horizons Forum and Aerospace Exposition*: American Institute of Aeronautics and Astronautics, 2011.

[18] Y.-b. Chen*, et al.*, "UAV path planning using artificial potential field method updated by optimal control theory," *International Journal of Systems Science,* pp. 37-41, 18 Jun 2014 2014.

[19] S. Srikanthakumar*, et al.*, "Optimization-Based Safety Analysis of Obstacle Avoidance Systems for Unmanned Aerial Vehicles," *Journal of Intelligent & Robotic Systems,* vol. 65, pp. 219-231, 2012/01/01 2012.

[20] A. Mark and R. Andrew, "Formation flight as a cooperative game," in *Guidance, Navigation, and Control Conference and Exhibit*: American Institute of Aeronautics and Astronautics, 1998.

[21] M. Niculescu, "Lateral track control law for Aerosonde UAV," in 39th AIAA Aerospace Sciences Meeting and Exhibit, 2001.